ELSEVIER

Chemical Engineering Journal 86 (2002) 85–93

Chemical Engineering Journal

www.elsevier.com/locate/cej

Simultaneous moisture transport and shrinkage during drying of solids with ellipsoidal configuration

A.G.B. de Lima [a,*], M.R. Queiroz [b], S.A. Nebra [c]

[a] Departamento de Engenharia Mecânica, CCT, Universidade Federal da Paraíba (UFPB), Av. Aprígio Veloso, 882, CEP 58109-970, Caixa Postal 10069, Campinas Grande-PB, Brazil

[b] Depto. de Pré-Processamento de Produtos Agropecuários, FEAGRI, Universidade Estadual de Campinas (UNICAMP), Campinas-SP, Brazil

[c] Departamento de Energia, FEM, Universidade Estadual de Campinas (UNICAMP), CEP 13083-970, Caixa Postal 6122, Campinas-SP, Brazil

Abstract

This work presents a two-dimensional diffusional model to predict the simultaneous mass transfer and shrinkage during drying of solids with prolate spheroidal shape, considering that the changes in volume of solid are equal to the volume of evaporated water. The resulting equations are numerically solved, using the finite-volume method. This model was used to study numerically the effect of the air-drying conditions and shrinkage on the drying kinetic of banana peel for six experiments, considering the natural shape of this fruit. Here, it was treated as an ellipsoid of revolution. Several results are shown and analyzed such as the comparison between numerical and experimental data; the dimensionless shrinkage parameters; the relationships of length, superficial area and volume; the moisture content distribution and finally the mass transfer and diffusion coefficients.

Keywords: Drying; Simulation; Mass; Shrinkage; Ellipsoidal geometry; Banana

1. Introduction

Fresh fruits and vegetables are dried after harvesting in order to reduce waste and spoilage and to extend their shelf life. During dehydration of foods, drying of fruits and vegetables produces great changes in their volume and surface area simultaneously with loss of moisture. Therefore, it is necessary to devote more attention to the shrinkage phenomenon, because it affects the drying rate and diffusion coefficient.

Engineers and researchers have produced several theoretical and experimental studies to predict mass transfer of foods, in particular the banana-drying process [1–9]. However, not much works has been done on moisture diffusion behavior including shrinkage [10–13]. These reports that the following conclusions may summarize the phenomenon which produces a great influence on the drying rate, modifying the diffusion coefficient sufficiently [10,11]: the drying rate decreases with the increase in the length of samples used in the drying experiments [12]; and the volume-shrinkage coefficient approximates unity for all drying methods except freeze drying, for which it is much lower [13]. In all studies cited above, the diffusion model was used considering single geometry such as plate or cylinder.

The objectives of this work are: (a) to develop a mathematical model for simulating simultaneous moisture transport and shrinkage of prolate spheroidal solids (Fig. 1); (b) to study numerically the effect of the air drying conditions and shrinkage on the drying of peeled banana and (c) to calculate the mass transfer and effective diffusion coefficients of banana under six air-drying conditions.

2. Theoretical analysis

The assumptions used in the mathematical model are:

(a) the shape of banana is approximates to an ellipsoid of revolution;
(b) the shrinkage of the solid is equal to the volume of water evaporated;
(c) the shrinkage is two-dimensional and axi-symmetric around z-axis;
(d) the drying occurs during the falling rate period;
(e) the unique mechanism of drying is diffusion;
(f) the moisture content is axi-symmetric around z-axis and constant at the beginning of the process;
(g) the thermo-physical properties are constant during the drying process;

* Corresponding author.
E-mail addresses: gilson@dem.ufpb.br (A.G.B. de Lima), marlene@agri.unicamp.br (M.R. Queiroz), sanebra@fem.unicamp.br (S.A. Nebra).

1385-8947/02/$ – see front matter
PII: S1385-8947(01)00276-5

Nomenclature

$Bi_{\rm m}$	Biot number of mass transfer (–)
$\widehat{C}$	semi-perimeter of the banana (m)
D	diffusion coefficient (m^2/s)
ERMQ	least square error $(kg/kg)^2$
L	focal length (m)
L_1, L_2	minor and major axis of the solid (m)
M, $\bar{M}$	local and average moisture content (kg/kg)
N, S, E, W, P	nodal points (–)
S	area (m^2)
$\bar{S}^2$	variance (–)
t	time (s)
$t^*_{\rm m}$	Fourier number of mass transfer (–)
T	air temperature (°C)
UR	air relative humidity (–)
v	air velocity (m/s)
V	volume (m^3)
x, y, z	Cartesian coordinates (m)
Greek letters	
$\bar{\beta}$, $\bar{\beta}_1$, $\bar{\beta}_2$	shrinkage coefficient (–)
Δ, δ	variation (–)
ξ, η, ζ	angular (⊥ x-axis), angular (⊥ z-axis) and radial coordinates (–)
Φ	function (–)
∇	gradient (–)
Subscripts	
e	equilibrium
e, w, s, n	boundary of the nodal points
0	initial
Superscripts	
*	dimensionless
o	old
t	time

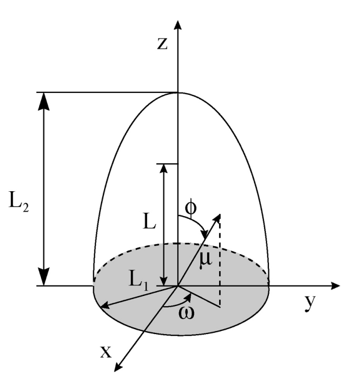

Fig. 1. Prolate spheroidal solid.

(h) at the surface material, convective boundary conditions are used;
(i) the solid is composed of water in liquid phase and solid material.

Based on these assumptions, the following equations were developed to simulate the shrinkage and diffusion phenomenon simultaneously. Fig. 1 shows the coordinate system used in this work.

2.1. Liquid diffusion model

The following dimensionless parameters are used:

$$M^* = \frac{M - M_{\rm e}}{M_0 - M_{\rm e}}, \qquad \eta^* = \eta, \qquad \xi^* = \xi,$$
$$t^*_{\rm m} = \frac{Dt}{L^2}, \qquad V^* = \frac{V}{L^3}, \qquad Bi_{\rm m} = \frac{h_{\rm m}L}{D} \tag{1}$$

Fick's second law for liquid diffusion in prolate spheroidal coordinates (ξ, η, ζ) using dimensionless parameters, considering symmetry around z-axis, can be written as [14–18]

$$\frac{\partial M^*}{\partial t^*_{\rm m}} = \frac{1}{\xi^{*2} - \eta^{*2}}\left[\frac{\partial}{\partial \xi^*}\left((\xi^{*2} - 1)\frac{\partial M^*}{\partial \xi^*}\right)\right] + \frac{1}{(\xi^{*2} - \eta^{*2})}\left[\frac{\partial}{\partial \eta^*}\left((1 - \eta^{*2})\frac{\partial M^*}{\partial \eta^*}\right)\right] \tag{2}$$

with the following initial and boundary conditions:

$$t = 0, \qquad M^*(\xi^*; \eta^*; 0) = 1 \tag{3a}$$

$$t > 0, \qquad M^*\left(\xi^* = \frac{L_2}{L}; \eta^*, t^*_{\rm m}\right) = -\frac{1}{Bi_{\rm m}}\sqrt{\frac{(\xi^{*2} - 1)}{(\xi^{*2} - \eta^{*2})}}\left.\frac{\partial M^*}{\partial \xi^*}\right|_{\xi = L_2/L} \tag{3b}$$

2.2. Shrinkage model

A fundamental point in the shrinkage model is the inclusion of an equation that relates volume and average moisture content. The following relation for linear shrinkage was proposed:

$$(V)_t = V_0(\bar{\beta}_1 + \bar{\beta}_2\bar{M}) \tag{4}$$

Since $t = 0 \Rightarrow \bar{M} = \bar{M}_0$ and $(V)_{t=0} = V_0$ and using the dimensionless parameters, we can write Eq. (4) as follows:

$$\frac{(V)^*_t}{V^*_0} = 1 - \bar{\beta}(\bar{M}^*_0 - \bar{M}^*) \tag{5}$$

with $\bar{\beta} = \bar{\beta}_2(\bar{M}_0 - \bar{M}_{\rm e})$. When $\bar{\beta} = \bar{\beta}_2 = 0$, we have the case without shrinkage.

The volume of ellipsoid is given by [19]:

$$(V)_t = \tfrac{4}{3}\pi(L_2)_t(L_1)^2_t \tag{6}$$

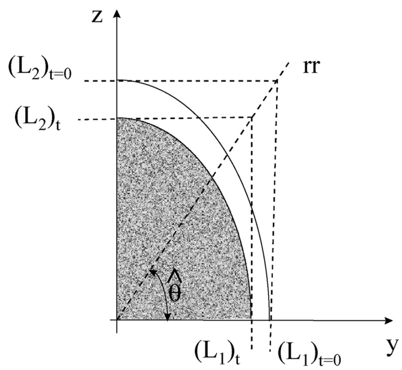

Fig. 2. Shrinkage of the prolate spheroidal solid during diffusion process.

From Fig. 2, it can be verified that

$$\left(\frac{L_2}{L_1}\right)_t = \left(\frac{L_2}{L_1}\right)_{t=0} = \mathrm{Tg}\hat{\theta} \tag{7}$$

Using Eqs. (5)–(7), the new dimensions of the body are determined along with the time. In this case, the superficial area of the prolate spheroid may be calculated as follows [20]:

$$(S)_t = 2\pi (L_1)_t (L_2)_t \times \left\{ \frac{(L_1)_t}{(L_2)_t} + \frac{\arcsin[\sqrt{[1-((L_1)_t/(L_2)_t)^2]}]}{\sqrt{[1-((L_1)_t/(L_2)_t)^2]}} \right\} \tag{8}$$

2.3. Diffusion and mass transfer coefficients

The diffusion and mass transfer coefficients were estimated using the least square error technique and variance, as follows:

$$\mathrm{ERMQ} = \sum_{i=1}^{n} (\bar{M}^*_{i,\mathrm{Num}} - \bar{M}^*_{i,\mathrm{Exp}})^2, \qquad \bar{S}^2 = \frac{\mathrm{ERMQ}}{(n-\hat{n})} \tag{9}$$

where n is the number of experimental points, and $\hat{n}$ is the parameters number fitted [21].

In order to estimate the fixed diffusion coefficient as a function of the air temperature, linear regression was made in an Arrhenius's equation using the software Statistica. This equation is given by

$$D = A_1 \, e^{-A_2/T} \tag{10}$$

where A_1 and A_2 are constants with appropriate dimensions.

3. Numerical methodology

Various numerical methods have been used to solve the problem of transient diffusion such as finite-difference, finite element, boundary element and finite-volume methods. In particular, in this work, the finite-volume method was used assuming fully implicit formulation and the practice B (nodal points at the center of the control volume) in a uniform grid size. In the simulation of diffusion phenomenon in prolate spheroids, a certain domain was utilized, due to the symmetry of the body. Details about the numerical procedure may be obtained in the literature [16,17].

4. Experimental methodology

4.1. Continuous experimental drying

The "Nanicão" variety of ripe banana (*Musa acuminata*, Cavendish subgroup), procured locally was used for the drying experiments. The fruits were selected according to the required degree of ripeness and peeled manually. Immediately after peeling, the fruits were dried with hot air under forced convection. Details of the procedure and the drying equipment used are reported in the literature [10,11]. Table 1 shows the air and material conditions used in this work.

4.2. Shrinkage

In order to determine the major external length (semi-perimeter) between the extremity, diameters (in two perpendicular directions) and the moisture content of the fruit along with the time, bananas peeled manually were disposed of in the oven under forced convection at a temperature of 70 °C.

Table 1
Air and banana experimental conditions used in this work

Test	Air			Banana					t (h)
	T (°C)	UR (%)	v (m/s)	M_0 (d.b.)	M_f (d.b.)	M_e (d.b.)	L_2 (m)	L_1 (m)	
1	29.9	35.7	0.38	3.43	0.32	0.1428	0.05856	0.01613	121.85
2	39.9	19.3	0.33	3.17	0.33	0.0664	0.05878	0.01569	72.00
3	49.9	19.2	0.37	3.21	0.32	0.0579	0.05901	0.01522	40.80
4	60.2	19.9	0.36	2.96	0.25	0.0426	0.05897	0.01530	35.30
5	60.5	10.7	0.35	3.04	0.31	0.0211	0.05909	0.01506	27.80
6	68.4	7.3	0.39	2.95	0.22	0.0121	0.05890	0.01545	27.60

The value of the L_2 (see Fig. 1) is obtained using the major external length of the fruit as follows:

$$\frac{\widehat{C}}{2} = L_2 \int_0^1 \sqrt{1 + \left(\frac{L_1}{L_2}\right)^2 \frac{\tilde{x}^2}{(1-\tilde{x}^2)}}\,\mathrm{d}\tilde{x}, \quad \text{with } \tilde{x} = \frac{z}{L_2} \tag{11}$$

The minor axis of the banana (L_1) was obtained by the arithmetic mean of the diameters measured. Details of the experimental and analytical procedures may be obtained in the literature [16]. In this way, the shrinkage coefficient $\bar{\beta}_2$ may be calculated by fitting Eq. (5) to the experimental data.

5. Results and discussions

5.1. Experimental shrinkage coefficient

The estimated value of the shrinkage coefficient in Eq. (5) applied to banana was $\bar{\beta}_2 = 0.269$, computed for moisture contents ranging from 3.16 to 0.34 kg/kg dry basis. The correlation coefficient was 0.99 and the ERMQ was 0.01120 [16]. The comparison curve between the shrinkage experimental and fitted data is shown in Fig. 3.

5.2. Drying kinetics of banana

Since the objective of this study was to develop a model applicable to the process of drying banana peels, the comparison of numerical and experimental data for six experiments are plotted in Figs. 4–9.

It is clearly seen in these figures that there was good agreement. Some discrepancies appear at low moisture content due to the fact that for longer drying time, the assumption of linear shrinkage is not valid, for a different manner as assumed in Eq. (5). The continuation of the numerical calculations for the test 6 permitted us to obtain the equilibrium moisture content of $\bar{M}^* = 7.97 \times 10^{-4}$ is approximately 64.15 h.

Table 2 presents the initial and final values of shrinkage parameters obtained during the banana-drying process for each experiment. When presented, the dimensionless shrinkage parameters $\bar{\beta}$ changes due to the dependence on the temperature and on initial and equilibrium moisture contents, in accordance with Eq. (5). It is observed that the relationships of length, superficial area and volume increase with the increase of air temperature as expected.

5.3. Moisture content distributions

The moisture content distribution inside the solid is very important in order to study the evolution of mechanical stress developed in the body due to the high moisture gradients. Fig. 10a–c shows the moisture content distribution inside the peeled banana exposed to the drying for 1.11, 5.00 and 15.00 h, respectively, for test 6. It can be seen in accordance with the iso-concentration lines, that the highest moisture gradients occur near the surface. There is also a close strong drying to the focal point. Thus these areas are more susceptible to have troubles such as cracks and fissures due to higher moisture gradients and shrinkage velocity.

Fig. 11 shows the moisture content distribution inside the peeled banana exposed to drying 15.00 h (test 3). By comparison with Fig. 10c, it is seen that the greatest moisture gradients are due to the smallest temperature; however, the drying occur slowly.

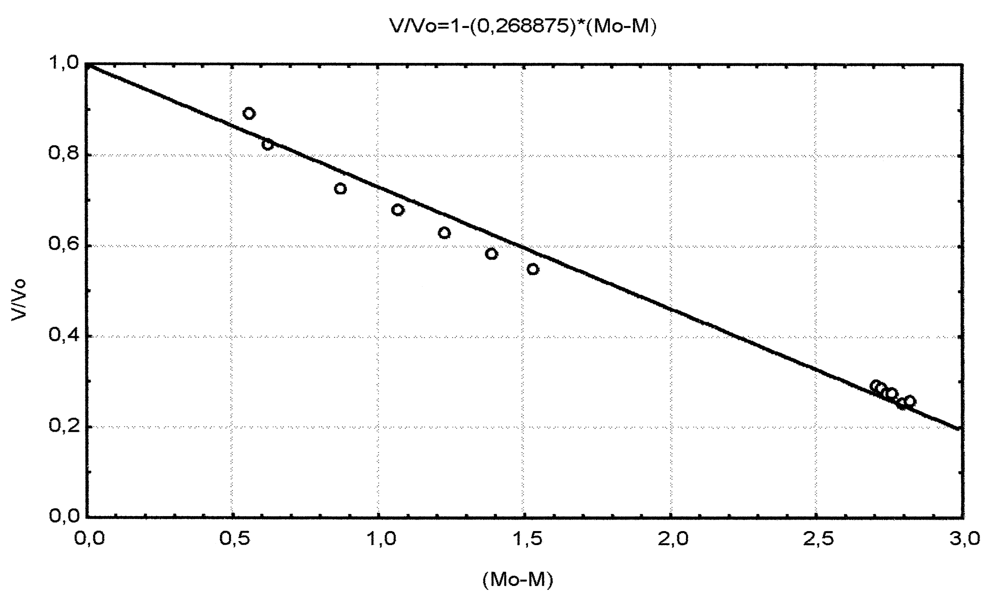

Fig. 3. Comparison between the experimental (○) and predicted volumes of banana obtained during the drying over to $T = 70\,^\circ\mathrm{C}$.

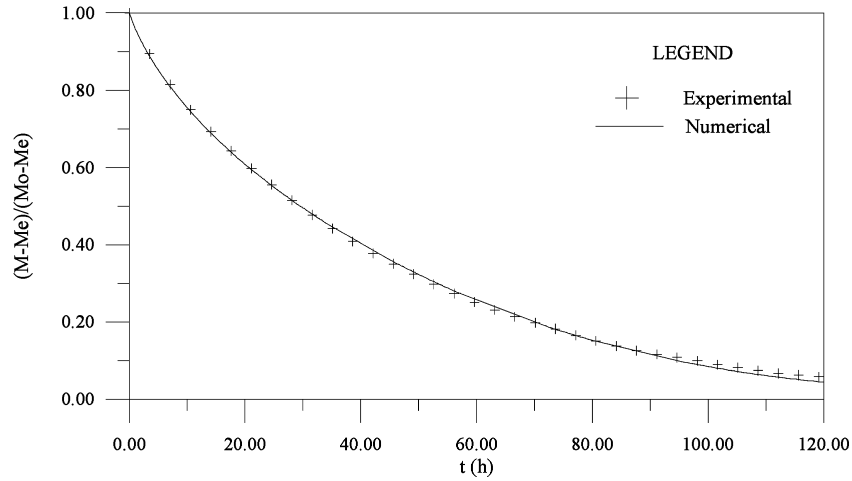

Fig. 4. Comparison between predicted and experimental dimensionless mean moisture content during the drying of banana (test 1).

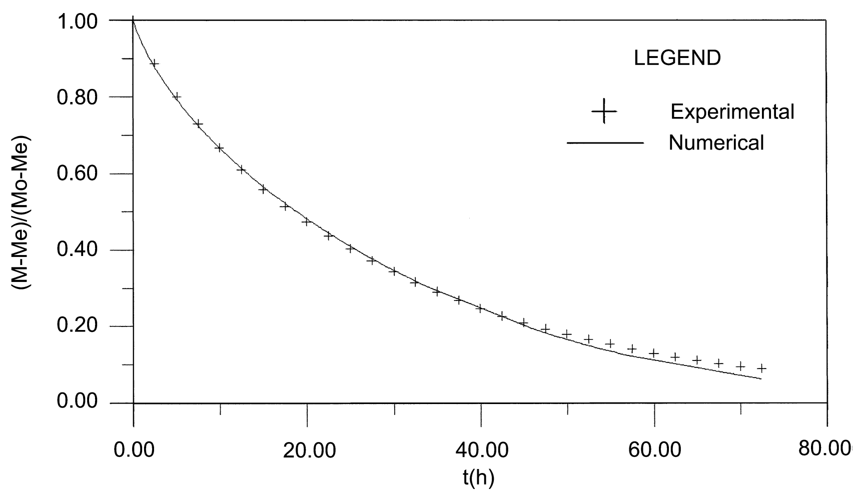

Fig. 5. Comparison between predicted and experimental dimensionless mean moisture content during the drying of banana (test 2).

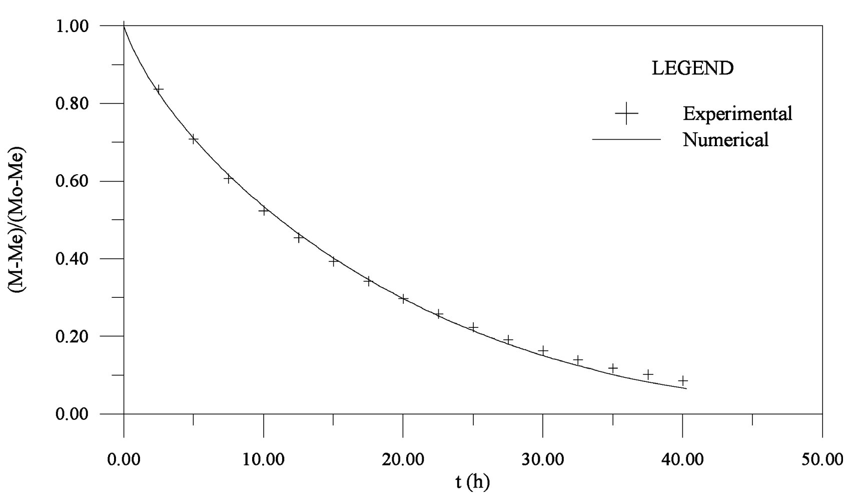

Fig. 6. Comparison between predicted and experimental dimensionless mean moisture content during the drying of banana (test 3).

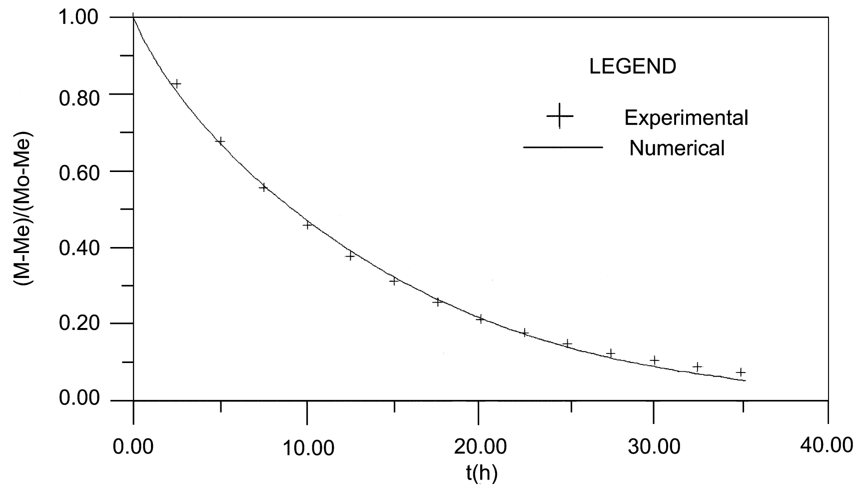

Fig. 7. Comparison between predicted and experimental dimensionless mean moisture content during the drying of banana (test 4).

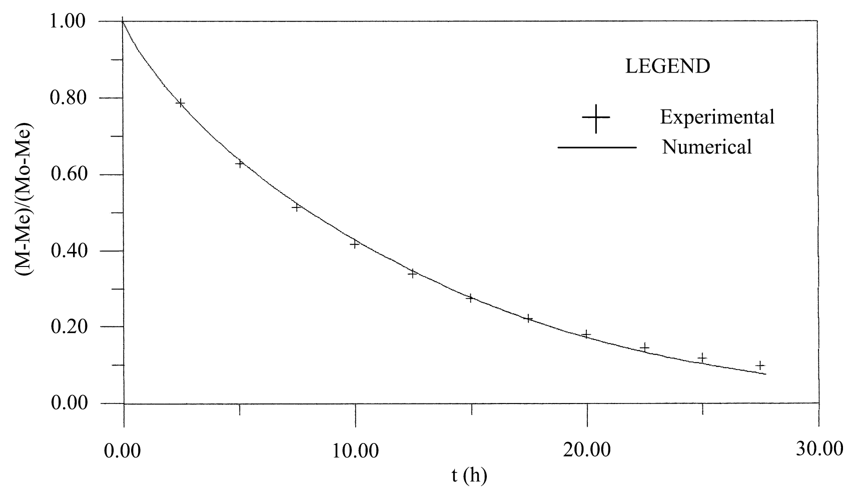

Fig. 8. Comparison between predicted and experimental dimensionless mean moisture content during the drying of banana (test 5).

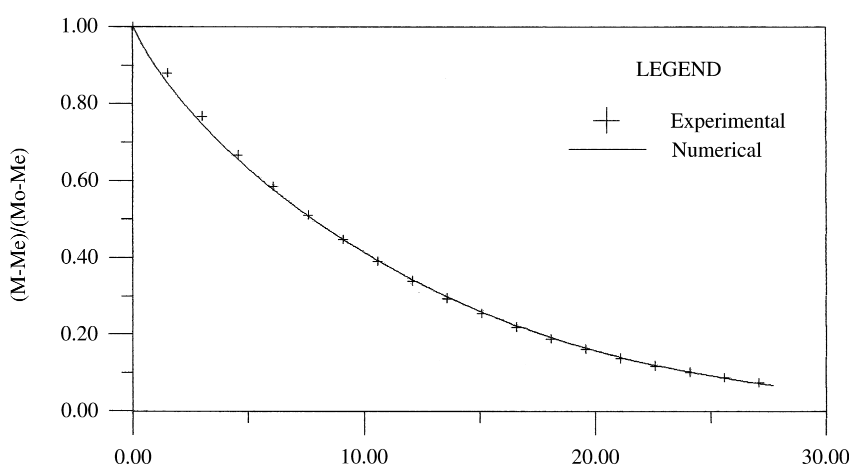

Fig. 9. Comparison between predicted and experimental dimensionless mean moisture content during the drying of banana (test 6).

Table 2
Dimensionless shrinkage coefficient and dimensions of the peeled banana during the drying

Test	Initial				Final				$\bar{\beta}$
	L_1 (cm)	L_2 (cm)	V (cm^3)	S (cm^2)	L_1 (cm)	L_2 (cm)	V (cm^3)	S (cm^2)	
1	1.6130	5.8562	63.822	96.099	0.8614	3.1274	9.720	27.407	0.8838
2	1.5690	5.8784	60.616	93.676	0.9457	3.5433	13.275	34.035	0.8345
3	1.5220	5.9016	57.265	91.074	0.9001	3.4903	11.846	31.856	0.8475
4	1.530	5.8977	57.830	91.518	0.9729	3.7503	14.869	37.006	0.7844
5	1.5060	5.9095	56.142	90.184	0.9481	3.7205	14.010	35.746	0.8117
6	1.5450	5.8903	58.896	92.349	0.9915	3.7800	15.565	38.032	0.7899

5.4. Diffusion coefficient

Table 3 presents the transport coefficients as well as the variance obtained for all experiments. In this table, the two values of Biot number refer to the initial and final values of this parameter during drying. The highest internal resistance to moisture is comes from the lowest temperature. The small variance indicates that the model agrees well with the experimental data. As expected, all the transport coefficients increases strongly with the temperature. Table 4 presents the values of the constants in accordance with the equation.

In general, comparison between the diffusion coefficients reported in the literature is difficult due to the different

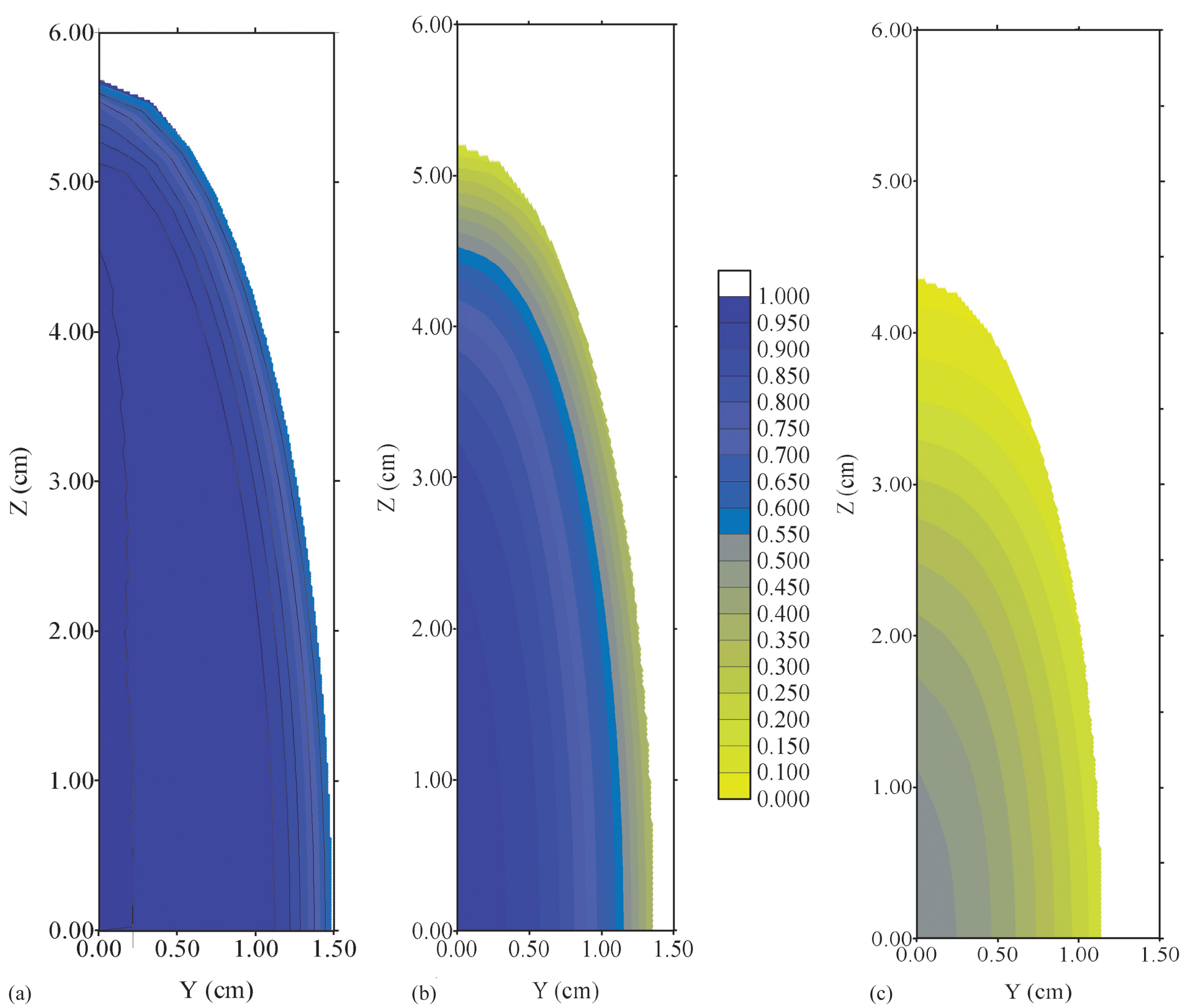

Fig. 10. Dimensionless moisture content distribution (M^*) inside the banana peel (test 6): (a) $t = 1.11$ h; (b) $t = 5.00$ h; (c) $t = 15.00$ h.

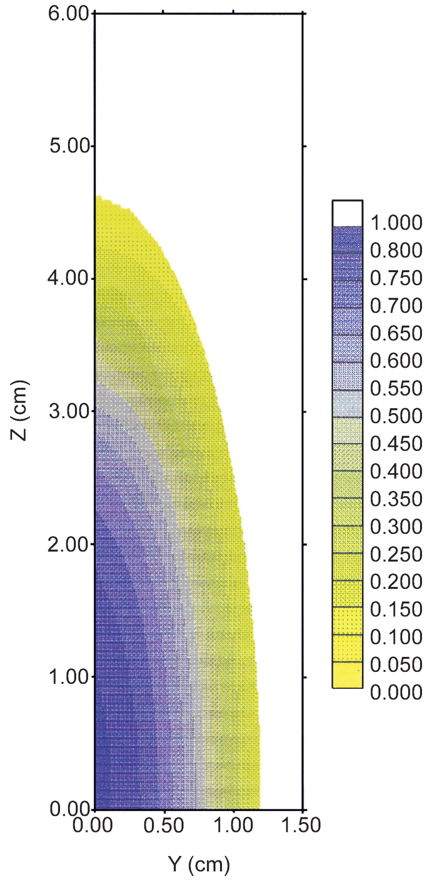

Fig. 11. Dimensionless moisture content distribution (M^*) inside the banana for elapsed time from $t = 15.00$ h (test 3).

Table 3
Transport coefficients estimated and variance for all drying experiments

Test	$D \times 10^{10}$ (m^2/s)	$h_m \times 10^8$ (m/s)	Bi_m	$\bar{S}^2 \times 10^4$
1	1.65	10.10	34.46, 18.40	0.96
2	2.48	15.53	35.47, 21.38	1.20
3	4.57	21.35	26.64, 15.75	0.91
4	7.25	22.30	17.52, 11.14	0.68
5	7.30	26.15	20.47, 12.89	1.48
6	8.63	26.56	17.49, 11.23	1.42

Table 4
Coefficients A_i of Eq. (10) and the values of R, and $\bar{S}^2$

$A_1 \times 10^{10}$ (m^2/s)	A_2 (K)	R	$\bar{S}^2$
2448930.845	−4265.277	0.9871	0.2092

models and calculation methods used, and also due to unlike composition and physical and chemical structure of the material. However, by comparing the mass diffusivity values of banana–water system obtained in this study with others, reported in Table 5, it was observed to be in reasonable concordance. As the diffusive model was used in all works reported in Table 5, the difference between the values may be attributed mainly to the following factors: dehydration method, product variety; geometry assumptions; different equilibrium moisture content hysteresis phenomenon in the sorption isotherm); boundary conditions; product physical structure and shrinkage effects (probable formation of the porous, by water evaporation).

Some authors neglect the effects of the external resistance and/or shrinkage during the modeling and implicitly consider these effects in the diffusion coefficient. The value of the diffusion coefficient predicted this manner is smallest that the presented in Table 3, for a same drying condition [22].

As a final comment, it can be said that although valuable results have been obtained from this study, it is necessary to pay more attention to the quantitative study of superficial area and volume changes during the dehydration processes, especially in complex situations such as multi-directional deformations, and temperature changes occur simultaneously. Multi-directional deformations occur in the drying of some fruits such as grape or fig where at the end of the process, the product is totally wrinkled.

Table 5
Moisture diffusivity of banana for several temperatures and shapes

Shape (assumption)	M^a (d.b.)	T (°C)	$D \times 10^{10}$ (m^2/s)	References
Pieces (semi-infinite plate)	0.027	25	0.0251	[23]
Complete peeled (infinite cylinder)	3.77–0.06	50–70	2.62–6.53	[24,25]
–	3.50–0.01	20–40	0.003–2.10	[26]
Slices (plate)	2.10	60	34.80 (free 15°Brix)	[27]
	0.20		8.80 (39°Brix)	
Complete peeled (infinite cylinder)	3.43–0.22	29.9–68.4	1.25, 29.7	[10,11]
Cylindrical pieces	2.64–1.85	25–45	8.50–24.30	[7]
Slices (finite cylinder)	Initial: 3.20–2.39	35–50	1.60–4.80	[1]
	Final: 0.89–0.28			
Cubes	3.54–0.11	60	8.33	[28]
Slices	3.00–0.15		2.80–163.40	[29]
Slices (plate)	–	50	27.7 (60°Brix)	[30]
			26.6 (70°Brix)	

[a] The range of the values refers to the initial and final moisture content of the fruit.

6. Conclusions

Fundamental equations for the liquid diffusion in prolate spheroidal bodies, considering shrinkage effect, were developed. The finite-volume method was used to solve the equations applied to the banana drying process.

From the results the following can be concluded. (a) The model and the technical used has great potential and it is accurate and efficient to simulate many practical problems of diffusion such as heating, cooling, wetting and drying in prolate spheroidal solids, including spheres as limit case. (b) Data of length, superficial area and volume and dimensionless linear shrinkage coefficient of banana for different temperatures are presented The dimensionless linear shrinkage coefficient changes with the temperature. (c) The diffusion coefficients increases strongly with the increase of the temperature, changing from 1.65×10^{-10} m^2/s at 29.9 °C to 8.63×10^{-10} m^2/s at 68.4 °C. (d) Highest moisture gradients in the banana are found near the surface and around the focal point.

This model can be adapted to describe drying process in material with variable properties, when it is almost impossible to obtain an analytical solution, and in cases with other boundary conditions under small modifications.

Acknowledgements

The authors would like to express their thanks to CAPES (Coordenação de Aperfeiçoamento de Pessoal de Nivel Superior, Brazil) and CNPq (Conselho Nacional de Desenvolvimento Científico e Tecnológico) for their financial support to this work.

References

[1] M.A. Mauro, F.C. Menegalli, Evaluation of diffusion coefficients in osmotic concentration of bananas (*Musa* Cavendish Lambert), Int. J. Food Sci. Technol. 30 (1995) 199–213.
[2] P. Schirmer, S. Janjai, A. Esper, R. Smitabhindu, W. Mühlbauer, Experimental investigation of the performance of the solar tunnel dryer for drying bananas, Renew. Energy 7 (2) (1996) 119–129.
[3] A.E. Drouzas, H. Schubert, Microwave application in vacuum drying of fruits, J. Food Eng. 28 (1996) 203–209.
[4] C.T. Kiranoudis, E. Tsami, Z.B. Maroulis, D. Marinos-Kouris, Drying kinetics of some fruits, Drying Technol. 15 (5) (1997) 1399–1418.
[5] R.G. Bowkey, K.A. Buckle, I. Hamey, P. Pavenayotin, Use of solar energy for banana drying, Food Technol. Aust. 32 (6) (1980) 290–291.
[6] M.K. Krokida, E. Tsami, Z.B. Maroulis, Kinetics on color changes during drying of some fruits and vegetables, Drying Technol. 16 (1–2) (1998) 667–685.
[7] N.K. Rastogi, K.S.M.S. Raghavarao, K. Niranjan, Mass transfer during osmotic dehydration of banana: Fickian diffusion in cylindrical configuration, J. Food Eng. 31 (1997) 423–432.
[8] M.K. Krokida, Z.B. Maroulis, D. Marinos-Kouris, Effect of drying methods on physical properties of dehydrated products, in: Proceedings of the International Drying Symposium (IDS'98), Vol. VA, Halkidiki, Greece, 1998, pp. 809–816.
[9] S. Prasertsan, P. Saen-sabv, Heat pump drying of agricultural materials, Drying Technol. 16 (1–2) (1998) 235–250.
[10] M.R. Queiroz, Theoretical and experimental study of the drying kinetics of banana, Doctor Thesis, State University of Campinas, Campinas, Brazil, 1994, 176 pp. (in Portuguese).
[11] M.R. Queiroz, S.A. Nebra, Theoretical and experimental analysis of the drying kinetics of bananas, in: Proceedings of the 10th International Drying Symposium (IDS'96), Part B, 1996, pp. 1045–1052.
[12] S.A. Coutinho, O.L.S. Alsina, O.S. Silva, Effect of the thickness in the drying of banana in monolayer, 2° Congresso Brasileiro de Engenharia Química em Iniciação Científica, Uberlândia, Brazil, Vol. 1, 1997, pp. 215–218 (in Portuguese).
[13] M.K. Krokida, Z.B. Maroulis, Effect of drying method on shrinkage and porosity, Drying Technol. 15 (10) (1997) 2441–2458.
[14] A.G.B. Lima, S.A. Nebra, C.A.C. Altemani, Simulation of the drying kinetics of the silkworm cocoon considering diffusive mechanism in elliptical coordinate, in: Proceedings of the Inter-American Drying Conference (IADC), Part B, Itu, Brazil, 1997, pp. 317–324.
[15] A.G.B. Lima, S.A. Nebra, The finite-volume approach for the solution of the transient diffusion equation applied to prolate spheroidal solids, in: Proceedings of the 15th Brazilian Congress of Mechanical Engineering (COBEM'99), Vol. 1, Águas de Lindóia, Brazil, CD-ROM, 1999.
[16] A.G.B. Lima, Diffusion phenomenon in prolate spheroidal solids, case studies: drying of banana, Doctor Thesis, State University of Campinas, Campinas, Brazil, 1999 (in Portuguese).
[17] A.G.B. Lima, S.A. Nebra, Theoretical analysis of the diffusion process inside prolate spheroidal solids, Drying Technol. 18 (1–2) (2000) 21–48.
[18] A.G.B. Lima, S.A. Nebra, Theoretical study of intermittent drying (tempering) in prolate spheroidal bodies, in: Proceedings of the International Drying Symposium (IDS'2000), Halkidiki, The Netherlands, 2000, CD-ROM.
[19] F. Provenza, in: F. Provenza (Ed.), Projetista de Máquinas, São Paulo, 1989, p. 2.47.
[20] G. Pólya, G. Szegö, Inequalities for the capacity of a condenser, Am. J. Math. V LXVII (1945) 1–32.
[21] R.S. Figliola, D.E. Beasley, Theory and Design for Mechanical Measurements, Wiley, New York, 1995, 607 pp.
[22] G.K. Vagena, D. Marinos-Kouris, Drying kinetics of apricots, Drying Technol. 9 (3) (1991) 735–752.
[23] Y.C. Hong, A.S. Bakshi, T.P. Labuza, Finite element modelling of moisture transfer during storage of mixed multicomponent dried foods, J. Food Sci. 51 (3) (1986) 554–558.
[24] R.I. Nogueira, Processo de secagem de banana (*Musa acuminata* subgrupo Cavendish cultivar nanica) parâmetros ótimos na obtenção de banana-passa, Master Thesis, State University of Campinas, Campinas, Brazil, 1991.
[25] R.I. Nogueira, K.J. Park, Drying parameters to obtain "banana-passa", in: Proceedings of the International Drying Symposium (IDS'92), Part A, Montreal, Canada, 1992, pp. 874–883.
[26] N. Kenchaou, M. Maalej, Evaluation of diffusion coefficient in the case of banana drying, in: Proceedings of the Ninth International Drying Symposium (IDS'94), Vol. VB, 1994, pp. 841–848.
[27] C.K. Sankat, C.R. Maharaj, The air-drying behavior of fresh and osmotically dehydrated banana slices, Int. J. Food Sci. Technol. 31 (1996) 123–135.
[28] G. Mowlah, K. Takano, I. Kamoi, T. Obara, Water transport mechanism and some aspects of quality changes during air dehydration of bananas, Lebensmittel-Wissenschaft Technol. 16 (1983) 103–107.
[29] R. Garcia, F. Leal, C. Rolz, Drying of bananas using microwave and air ovens, Int. J. Food Sci. Technol. 23 (1988) 73–80.
[30] K.N. Waliszewski, M.A. Salgado, M.A. Garcia, Mass transfer in banana chips during osmotic dehydration, Drying Technol. 15 (10) (1997) 2597–2607.